ANALYSIS OF WAVE CLIMATE TRENDS AND VARIABILITY

Val R. Swail[1]; Andrew T. Cox and Vincent J. Cardone[2]

1. INTRODUCTION

This paper describes the analysis of wave climate trends and variability from two long-term (40 years) wave hindcasts recently carried out by Environment Canada and Oceanweather. In this study, the NCEP/NCAR Reanalysis (NRA) surface (10 m) wind fields at six-hourly intervals were used to drive a global spectral ocean wave model for the 1958-1997 period. The detailed North Atlantic hindcast was based on kinematically reanalysed NRA wind fields, as described by Swail and Cox (1999). These enhanced wind fields were demonstrated to be a significant improvement over the NRA winds. A description of the evaluation of both hindcasts against in situ and satellite data is given in this publication by Cox *et al.* (2003).

The issue of ocean wave variability and trend has been investigated in recent years by many researchers, using different data sets. Investigations using instrumental measurements in the North Atlantic were carried out by Carter and Draper (1988), and Bacon and Carter (1991, 1993). Bouws *et al.* (1996) studied operational wave analyses for ship routing prepared by the Koninklijk Nederlands Meteorologisch Instituut (KNMI). Gulev and Hasse (1999) used visual wave observations from voluntary observing ships. In recent years, several wave hindcast studies have been undertaken, including the Kushnir *et al.* (1997) ten-year hindcast of the North Atlantic, the Sterl *et al.* (1998) 15-year global hindcast based on the European Centre for Medium-range Weather Forecasts Reanalysis (ERA15), and the European Union Waves and Storms in the Atlantic (WASA) project 40-year hindcast of the Northeast Atlantic ocean (WASA, 1998). In general, all of these works showed an increase in significant wave height in the North Atlantic over the different periods, although details of the patterns and the magnitudes of the changes varied somewhat.

One disturbing property of earlier hindcast studies, and of real time NWP operations, is that changes over time in data sources, improvements in data analysis techniques and evolution and upgrades in numerical models have tended to impart a temporal or 'creeping' inhomogeneity into the real-time products of such centres. When the wind fields produced by these centres are used to drive a wave model, these creeping inhomogeneities are translated into the wave climate simulations. Therefore, output data quality varies over time and subtle changes in climate may be masked. By using the NRA wind fields (which were derived from one version of the NCEP model for the entire 40 years) as a base, much of the inhomogeneity should be removed. However, it also must be noted that the assimilation input changed with time, and this could still be a source of inhomogeneity. White (2000) noted that many trends in the NRA were correlated with the change in the number of observations. The largest impact was found in the southern hemisphere, and the North Atlantic is probably less influenced by changing data coverage. There are specific inhomogeneities in the North Atlantic as well, such as the termination of the Ocean Weather Ship programme in the early 1970s, that may have an inverse effect.

Fifteen statistics were computed for both the resultant wave heights and input wind fields on monthly, seasonal and annual time scales; trend and variability analysis was carried out for each grid point in both hindcasts. In addition,

1 Environment Canada, 4905 Dufferin Street, Downsview, Ontario, Canada M3H 5T4; e-mail: Val.Swail@ec.gc.ca
2 Oceanweather, Inc. 5 River Road, Cos Cob, CT 06807, USA

a spatial analysis was carried out for the northern hemisphere oceans relating the wave climate to the surface pressure patterns. The results of the two wave hindcasts were compared with each other, and with homogeneous point time series of waves to investigate potential biases in the trend analyses. The paper is organized as follows. Section 2 briefly describes the global and North Atlantic hindcasts. Section 3 provides a description of the wind and wave climate derived from each hindcast. Section 4 gives an assessment of the potential biases in the hindcast and in situ data. Section 5 contains our conclusions.

2. WAVE HINDCASTS

The global wave hindcast (GROW – Global Reanalysis of Waves) was carried out using Oceanweather's ODGP2 1-G fully discrete spectral wave model with a grid resolution of 2.5° longitude by 1.25° latitude. Wind fields are derived directly from the NCEP Reanalysis surface 10 m winds, updated at six-hourly intervals, and the model time step is three hours. The only modification to the wind fields in the global model was to convert them to effective neutral stability using the NRA 2 m temperature and sea surface temperature fields. Details of the selection of these particular NRA wind fields and their validation are given in Cardone *et al.* (2003; this publication). In the global model, ice fields were specified on a monthly basis, using long-term monthly historical ice concentration data. Details of the global hindcast methodology are given by Cox and Swail (2001).

The North Atlantic wave hindcast (AES40) was carried out using the ODGP 3-G wave model, with a grid resolution of 0.625° latitude by 1.25° longitude. The ice edge was based on the actual monthly ice concentration. The NRA wind fields were reanalysed and enhanced with the aid of analyst-interactive techniques, during which in situ data were correctly re-assimilated, wind fields in extratropical storms were intensified as necessary, and tropical cyclone boundary layer winds were included. Swail and Cox (1999) describe the generation of these wind fields in detail, and show the significant improvement in the reanalysed wave fields, particularly in the specification of storm peaks.

The wave height fields produced in this hindcast showed excellent agreement with in situ wave measurements and satellite wave estimates. Cox and Swail (2001) show detailed comparisons with the global hindcast, while Cox *et al.* (2003; this publication) show overall comparisons with both the global and detailed North Atlantic hindcasts.

3. CLIMATE ASSESSMENT

Fifteen statistics were computed for both the resultant wave heights and input wind fields on monthly, seasonal and annual time scales; trend and variability analysis was carried out for every grid point in each hindcast. Among the statistics computed were mean, standard deviation, skew, kurtosis, 50th, 90th, 95th and 99th percentiles, and exceedance above selected thresholds.

Figure 1 shows the mean annual wind speed and wave height distribution for the period 1958 to 1997 for the global (GROW) and North Atlantic (AES40) hindcasts. The maxima in the high-latitude areas in both hemispheres and along the prevailing storm tracks are very evident in these charts. It is interesting to note that wind speeds over land are far less than those over the oceans. As found by Sterl *et al.* (1998), the waves in the North Atlantic are higher than those in the North Pacific. There are no wave hindcast data poleward of 70° in either hemisphere in GROW, or north of 76°N in AES40.

Figure 2 shows the geographical distribution of the annual 99th percentile wind speed and wave height for each hindcast for 1958-1997. The patterns in both hindcasts are very similar to those of the means, although the areas of highest wind speed and wave height are even more accentuated. The areas of strongest winds in the GROW hindcast for the 99th percentile are between Iceland and Canada, while in the mean charts the Southern Ocean showed higher values. The 99th percentile GROW wind and wave charts do not reflect areas where episodic high winds and waves might be expected due to tropical storms, such as the south-eastern US coast and the Gulf of Mexico, the South China Sea, north Australia or the Indian Ocean. This is certainly due to the inability of the NRA to adequately resolve these relatively small atmospheric features.

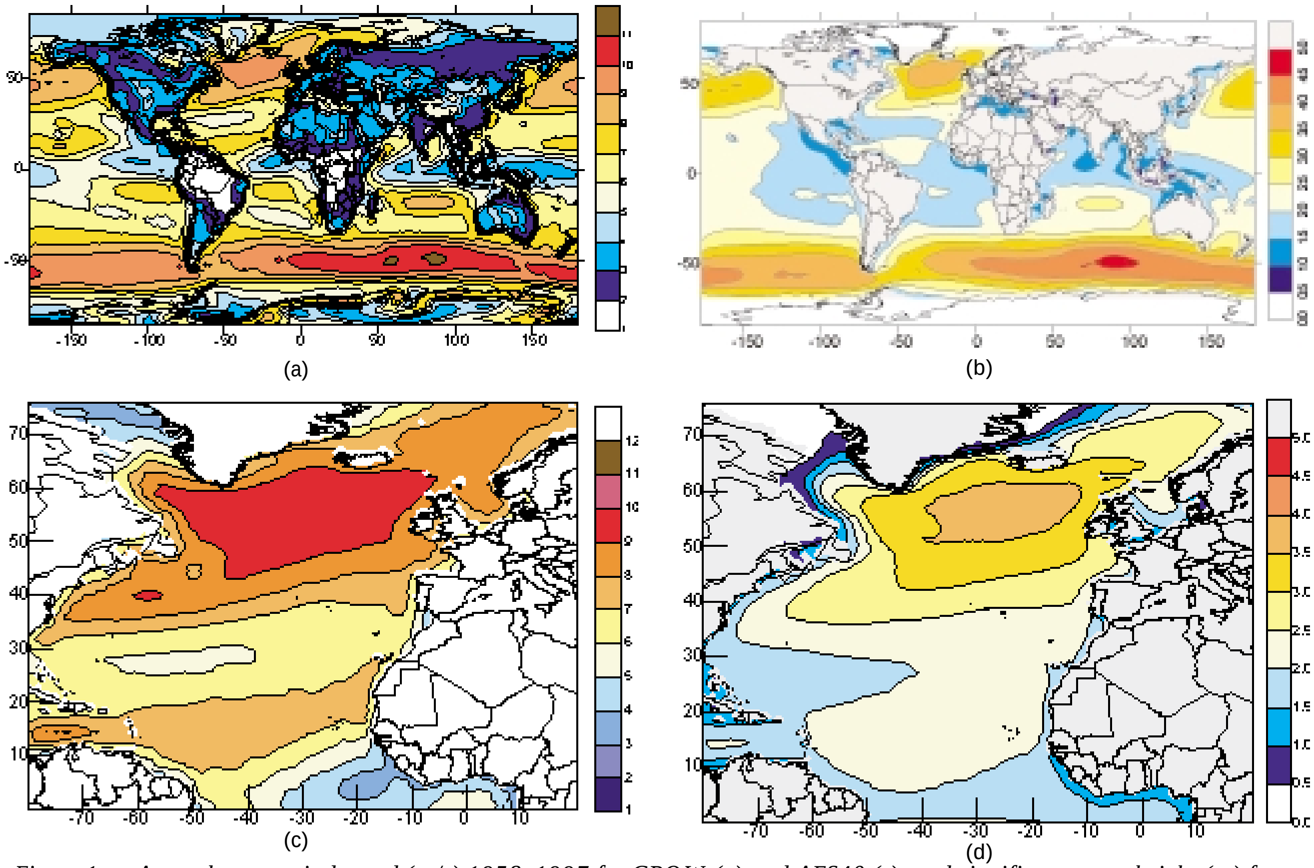

Figure 1 — Annual mean wind speed (m/s) 1958–1997 for GROW (a) and AES40 (c); and significant wave height (m) for GROW (b) and AES40 (d).

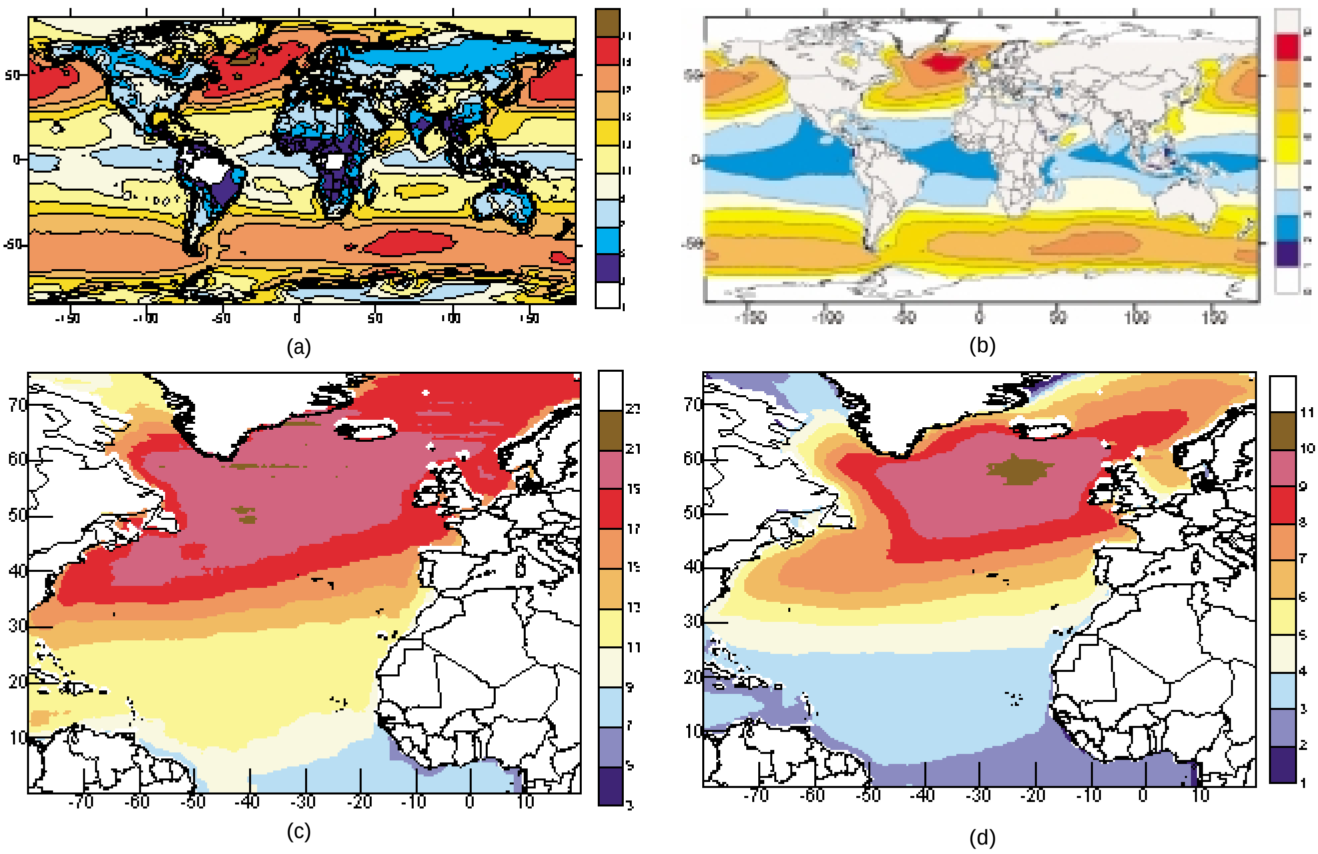

Figure 2 — 99th percentile wind speed (m/s) 1958–1997 for GROW (a) and AES40 (c); and significant wave height (m) for GROW (b) and AES40 (d).

A series of statistical analyses of the wind and wave trends was carried out for both hindcasts at each point on their respective grids. Trends were computed as simple linear trends over the 40 years of each hindcast using least squares fitting techniques. Figures 3 and 4 show the trends in the mean and 99th percentile wind speed and wave heights for the two hindcasts; trends are expressed as the inferred change over the 40-year period 1958-1997 based on the slope of the linear trend line. The areas where the null hypothesis (i.e. that the time series in question is random) is rejected at the 99 per cent level are also shown; the effect of series autocorrelation was also taken into account in determining the rejection levels. Increasing trends are most noticeable in the north-east Atlantic Ocean, across the northern edge of the North Pacific Ocean, and along the margins of Antarctica. The Antarctic trends are considered to be rather unreliable due to the data scarcity in the Southern Ocean as a whole, and documented problems in the NRA with the southern hemisphere, particularly south of 50°S. Negative trends in wave height are found mostly in equatorial regions, particularly in the Pacific Ocean, and also in the Labrador Sea. Particularly noticeable is the bi-polar nature of the trends in the North Atlantic, with strong increases in the north-east, and strong decreases in the south central North Atlantic. This pattern follows the dominant mode of the North Atlantic Oscillation. The spatial patterns of the trend in the mean and extreme (99th percentile) significant wave height are very similar. However, the magnitudes of the trends are much greater for the extreme wave heights than for the mean conditions, with large areas of increases in wave height of more than 1 m.

Wang and Swail (2001, 2002) describe in detail the results of spatial statistical analysis performed on both hindcasts; only a brief summary is included here. These studies used the Mann-Kendall test for trend against randomness at each grid point, accounting for autocorrelation; the time series were 'pre-whitened' and the autocorrelation and regressions coefficients were computed using an iterative scheme. Redundancy analysis techniques (described by Wang *et al.*, 1999) were used to carry out detailed seasonal spatial statistical analyses for both the global and North Atlantic hindcasts. Like canonical correlation analysis (CCA), redundancy analysis is a technique used to associate patterns of variation in a predictor field with patterns of the predictand field through a regression model. It differs from CCA in that it seeks to find pairs of predictor and predictand patterns that maximize the associated predictand variance, rather than the correlation only. In the North Atlantic hindcast, significant increases in

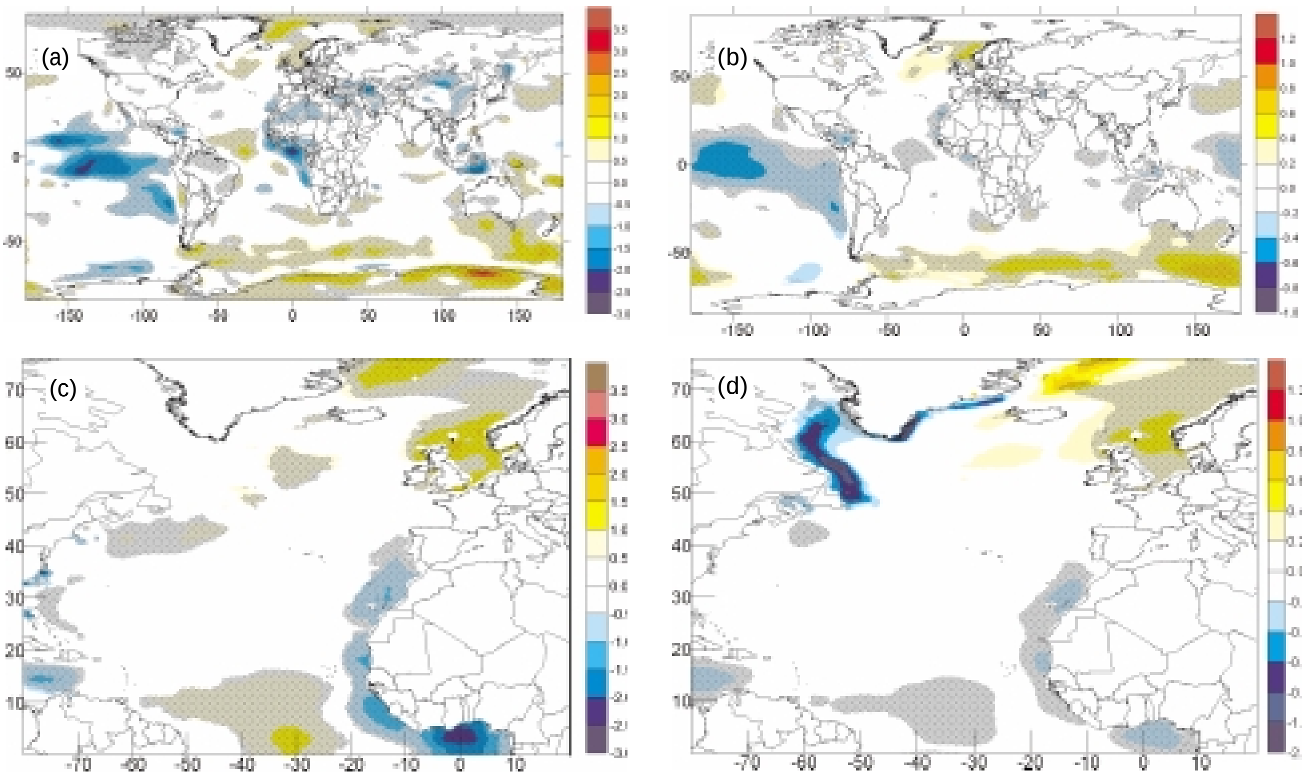

Figure 3 — Inferred change over the 1958–1997 period with 99 per cent statistical significance in annual mean wind speed (m/s) for GROW (a) and AES40 (c); and significant wave height (m) for GROW (b) and AES40 (d).

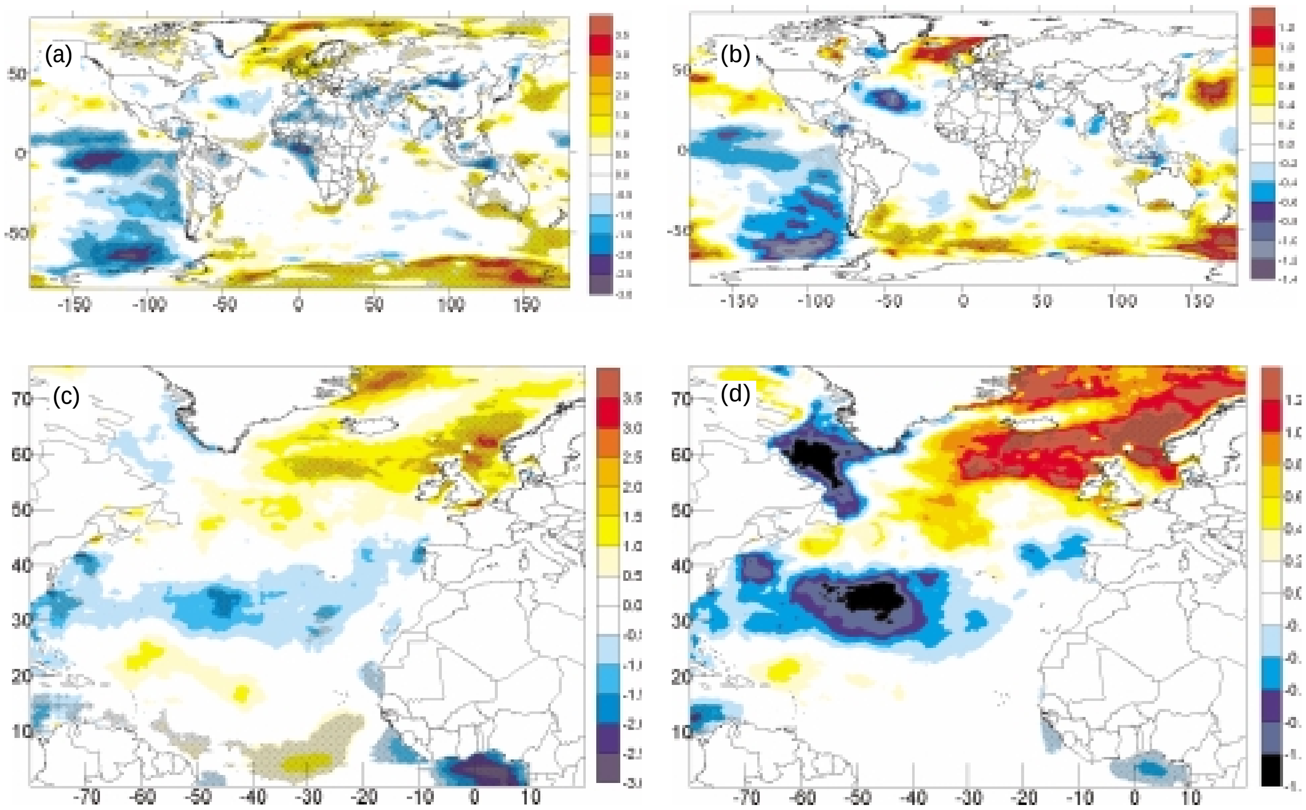

Figure 4 — Inferred change over the period 1958–1997 with 99 per cent statistical significance in annual 99th wind speed (m/s) for GROW (a) and AES40 (c); and significant wave height (m) for GROW (b) and AES40 (d).

the north-east Atlantic in the 90th percentile wave heights were matched by significant decreases in the subtropical North Atlantic, for the winter (JFM) season. The rates of increase/decrease are generally greater than those found in the global wave hindcast. Linear trends detected for the 99th percentiles are generally less significant than those for the 90th percentiles. The correlation between sea level pressure (SLP) and the 90th percentile wave height (H90) is significant at the 99th confidence level. Both time series possess a significant increasing trend at the 95 per cent confidence level, indicating that the Icelandic low has deepened during recent decades while the Azores high intensified, and, consequently, significant wave height (SWH) extremes have increased in the north-east NA, accompanied by decreases of SWH extremes in the subtropical NA. Both SLP and H90 are highly significantly correlated with the NAO index. Similar results were also found for winter (JFM) 99th percentile wave heights. In the global hindcast, changes in North Pacific winter (JFM) SWH are found to be significant at the 90 per cent confidence level; increases in SWH in the central North Pacific are found to be associated with a deepened and eastward extended Aleutian low. For both the North Atlantic and North Pacific, no significant trends of seasonal SWH extremes are found for the last century, though significant changes do exist in the last four decades; multi-decadal fluctuations are quite noticeable, especially in the North Pacific.

4. ASSESSMENT OF HOMOGENEITY

While the NRA used the same numerical prediction scheme for the 40-year period, thus removing the bias associated with ever-changing operational models, there still remain probable biases due to increased observational densities, and, particularly for ocean areas, an increase in shipboard anemometer heights coupled with an increased fraction of measured versus estimated winds. These are often referred to as ‘creeping inhomogeneities’, and are potentially serious constraints to any attempt to derive long-term trends. Therefore, we would like to verify the trend analyses derived from the two hindcasts against some long time histories of homogeneous measured data at selected points. Unfortunately, there exist very few locations in the global ocean where such data are available.

One location for which we do have reasonably homogeneous wind measurements over the 40-year period is at Sable Island, just off the east coast of Canada. We are also able to analyse the surface atmospheric pressure record from

Sable Island, along with records from two other sites in Nova Scotia (Halifax, Sydney) to compute pressure triangle wind records. As shown by Schmidt and von Storch (1993), the pressure triangle winds are most likely the least biased wind estimator available, since inhomogeneities in pressure records are much less than for most atmospheric variables.

Table 1 and Figure 5 show the trends for the Sable Island area from the hindcasts, Sable Island and the pressure triangle. In both the Sable Island measurements and the triangle winds, the trends in the percentiles are decreasing; the magnitude of the decreasing trend is comparable in both analyses, with the triangle wind trend being slightly more negative. The hindcast wind speed trends show a near-zero, but very slightly positive, trend. This most likely indicates an inhomogeneity introduced into the NRA winds. This could be a result of increased data densities in later years. For the NRA hindcast, it could also be a result of assimilating ship wind observations at an anemometer height of 10 m, when in fact the heights have increased from about 20 m at the beginning of the period to more than 30 m by the end of the period, with many observations coming from anemometers at heights exceeding 45 m. Coupled with an increase in the percentage of measured winds from ships, this could induce an artificial positive trend in the winds (and waves). In the 1990s, an increasing volume of moored buoy data would have been included in the NRA winds. These winds are taken at 5-m height, but are also assimilated at 10 m into the model. This would have the effect of reducing the wind speed trends, and thereby reducing, but not eliminating, the

Table 1—Summary of trends (per cent change/year) in winds and waves near Sable Island (1958-1997).

Per cent ILE	*NRA wind*	*AES40 wind*	*SABLE IS wind*	*TRIANGLE wind*	*SHIP wind*	*NRA wave*	*AES40 wave*
99	0.01	0.07	-0.12	-0.19	0.31	-0.01	0.15
90	0.03	0.09	-0.11	-0.14	0.13	-0.02	0.01
50	0.05	0.10	-0.24	-0.20	0.05	0.13	0.19

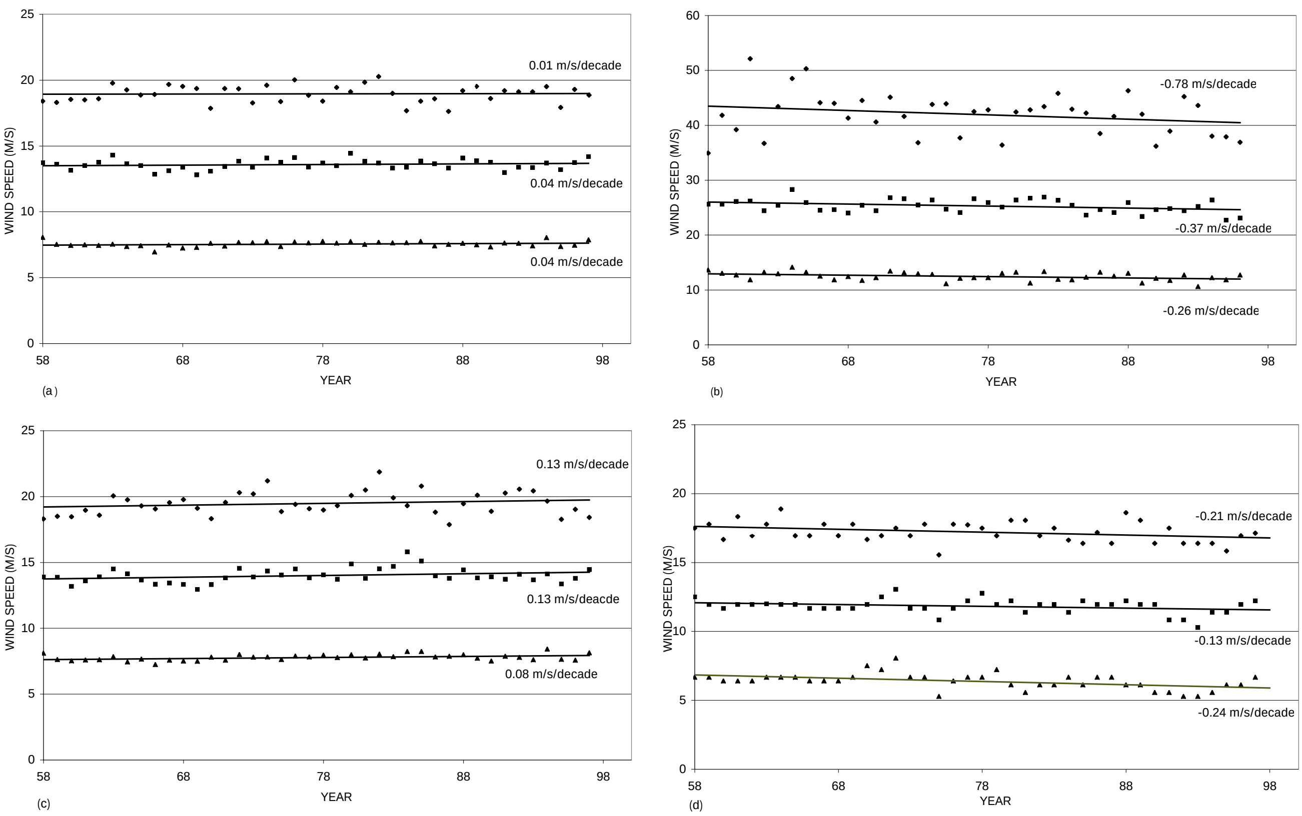

Figure 5 — Climate trends in 50th, 90th and 99th percentile wind speeds near Sable Island for (a) GROW, (b) pressure triangle, (c) AES40, (d) Sable Island measurements.

positive bias in areas near the buoys, i.e. we would expect the trends to be more positive if the buoy winds were assimilated at the correct heights. This is, in fact, what we see from the AES40 hindcast where both the ship winds and the buoy winds are assimilated at their actual anemometer heights. The AES40 trends in both winds and waves are consistently higher in this region, dominated by buoy observations in the 1990s, than the NRA trends. The AES40 trends should be a truer indication of the more intangible creeping inhomogeneities in the reanalysis process, such as increased data density, since the other sources, such as changing anemometer heights, have been mostly removed. Table 1 also shows the trends from Comprehensive Ocean-Atmosphere Data Set (COADS) ship observations. These wind speeds have been corrected where possible following the approach of Cardone *et al.* (1990). However, there remains a strong positive trend in wind speeds, particularly at the higher percentiles. Based on the Sable Island and triangle winds, this trend is most likely spurious, indicating that even these methods are unable to remove all of the artificial trend introduced by changing observational procedures on ships.

A second area for which 'ground truth' information is available for trends is off the Norwegian coast. WASA (1998) computed winds from two pressure triangles: (1) T-B-M (Thorshavn-Bergen-Mike (OWS)); and (2) T-A-B (Thorshavn-Aberdeen-Bergen). Table 2 and Figure 6 show the comparative results of the hindcasts and the WASA triangles. In this area both trends are positive, the hindcast winds being slightly more positive than the triangles. This indicates that the hindcast trends are reasonable, but probably slightly too high, or a good upper bound on real trends. Trends from adjusted ships in these areas similarly show increases in wind speed which are too strong, especially in the higher percentiles.

We have compared trends from ship wind observations in other areas with the hindcasts. In addition to the Sable Island box, and a box selected near the Hibernia oil field on the Grand Banks (47N, 47W), we have arbitrarily selected a mid-Atlantic 2° box (49N, 35W) and a box near the Bay of Biscay (45N, 9W). Table 3 shows that, except for the mid-Atlantic box, the adjusted ship trends show much larger increases than the hindcasts. It is also evident that the AES40 wind and wave trends are less than the NRA trends in the eastern Atlantic, while near Sable Island, where buoys dominate the later years, the AES40 trends exceed those from the NRA. Trends from the Labrador Sea, away from the influence of the buoys, show the same pattern as the eastern Atlantic. An anomaly appears for the Grand Banks, just outside the northern edge of the buoy coverage, where the AES40 wind trends exceed the NRA trends, but the AES40 wave trends are less.

Table 3 shows trend results from OWS Papa and OWS Bravo. Unfortunately, the overlapping period between the weathership records and the hindcasts is restricted to 24 years (Papa) and 16 years (Bravo). At Bravo, trends are negative for both the OWS and hindcasts. Consistent with a general artificial upward trend in hindcasts, the weathership trend is more negative (i.e. less positive). The same applies at the ship Papa location, although the OWS Papa trend looks somewhat suspicious, particularly the 99th percentile trend.

5. CONCLUSIONS

In this paper we have described the analysis of wave climate trend and variability from two ocean wave hindcasts: (1) a coarse mesh global hindcast based on wind

Table 2—Trends (per cent change/year) in winds and waves for WASA triangles, nearest hindcast points and 2° latitude-longitude adjusted COADS boxes (1958-1997).

	Per cent ILE	NRA wind	AES40 wind	WASA wind	SHIP wind	NRA wave	AES40 wave
TRIANGLE T-A-B	99	0.22	0.26		0.56	0.30	0.40
	90	0.28	0.28	0.23	0.44	0.40	0.44
	50	0.27	0.33		0.56	0.34	0.44
TRIANGLE T-B-M	99	0.29	0.34		0.73	0.45	0.54
	90	0.25	0.27	0.23	0.42	0.42	0.46
	50	0.22	0.30		-0.17	0.29	0.40

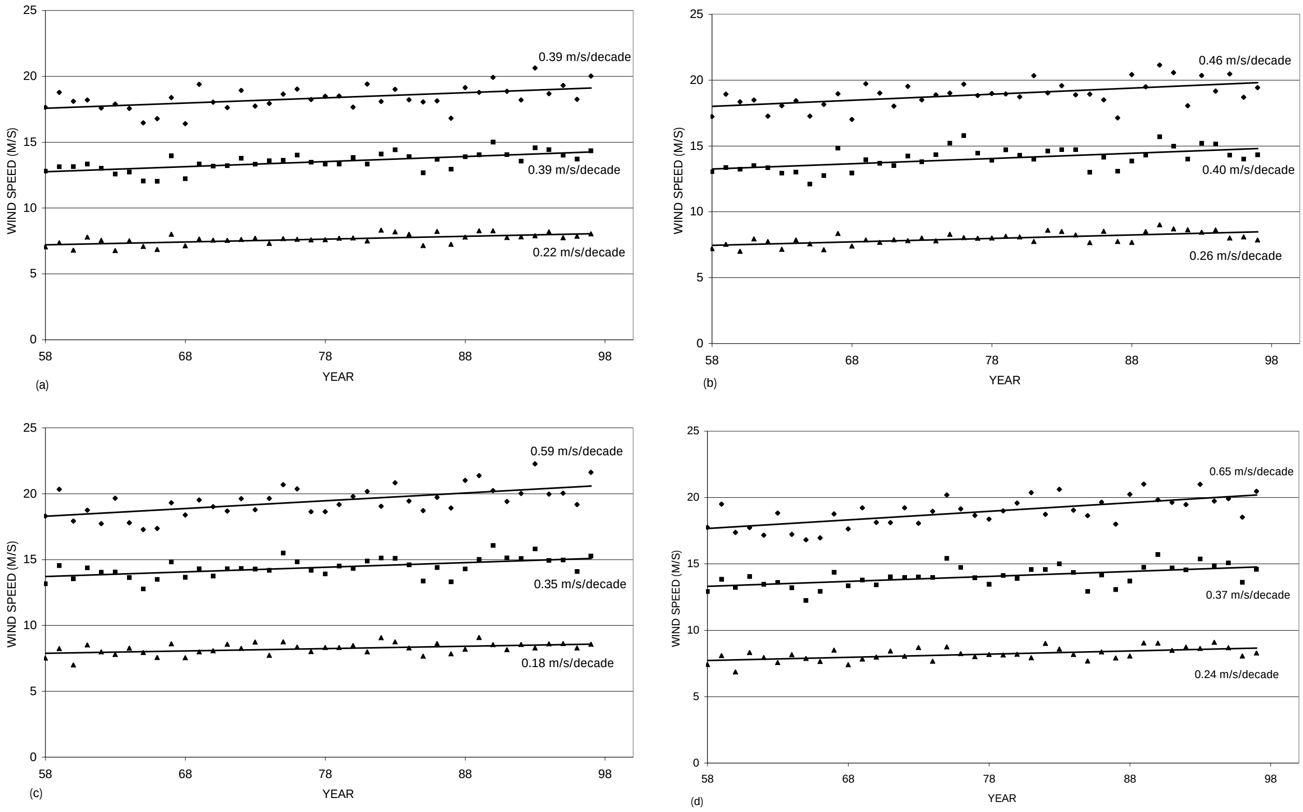

Figure 6 — Climate trends in 50th, 90th and 99th percentile wind speeds at eastern Atlantic pressure triangle locations: (a) triangle T-A-B (GROW); (b) triangle T-A-B (AES40); (c) triangle T-B-M (GROW); (d) triangle T-B-M (AES40).

Table 3—Trends (per cent change/year) in winds and waves at selected locations (1958-1997).

	Per centile	NRA wind	AES40 wind	SHIP wind	NRA wave	AES40 wave
SCOTIAN SHELF	99	0.01	0.07	0.31	-0.01	0.15
	90	0.03	0.09	0.13	-0.02	0.01
	50	0.05	0.10	0.05	0.13	0.20
GRAND BANKS	99	0.10	0.14	0.58	0.17	0.11
	90	0.13	0.18	0.53	0.07	-0.05
	50	0.14	0.17	0.41	0.09	-0.11
BAY OF BISCAY	99	-0.01	-0.03	0.32	0.03	-0.10
	90	-0.01	-0.04	0.16	-0.02	-0.06
	50	-0.02	-0.03	0.25	0.02	-0.02
MID-ATLANTIC	99	0.15	0.01	-0.05	0.17	0.18
	90	0.13	0.11	0.11	0.20	0.16
	50	0.11	0.11	-0.09	0.14	0.08
OWS BRAVO	99	-0.31	-0.64	-0.51	-0.64	-0.01
	90	-0.22	-0.35	-0.20	-0.35	-0.85
	50	-0.30	-0.30	-	-0.80	-0.99
OWS PAPA	99	-0.01	-	-0.94	-0.17	-
	90	-0.02	-	-0.46	0.06	-
	50	0.08	-		0.25	-

taken directly from the 40-year NCEP Reanalysis Project, and (2) a fine mesh hindcast of the North Atlantic Ocean based on manual kinematically reanalysed surface wind fields which have been shown to be significantly more representative in storm conditions. Each of these hindcasts has been analysed for trend. Both the global and North Atlantic trend analysis showed statistically significant areas of both increasing and decreasing winds and waves. The increasing trend in the north-east Atlantic and decreasing trend in the central north Atlantic are particularly well defined and consistent with reported changes in the NAO. Other increasing trends were found in the North Pacific in the global hindcast.

It is essential to verify trends derived from the modelled winds and waves with those computed from long-term homogeneous point time series of measured data. In the absence of such data in the southern hemisphere, we have low confidence in the rather large trends found in parts of the Southern Ocean. In the North Atlantic and North Pacific Oceans, the hindcast winds and waves appear to be affected by a creeping inhomogeneity due to the increased observational density. The global hindcast may be further affected by increasing anemometer heights on board ships, and the increased fraction of measured versus estimated ship winds. Nevertheless, the trends are generally consistent with the analysis of measurements from weather ships, transient ships, and the analysis of pressure triangle-derived geostrophic winds. This implies that the hindcasts may provide a good upper bound to true trends in the wind and wave climate.

REFERENCES

Bacon, S. and D.J.T. Carter, 1991: Wave climate changes in the North Atlantic and North Sea. *Int. J. Climatol.*, 11, 545-588.

Bacon, S. and D.J.T. Carter, 1993: A connection between mean wave height and atmospheric pressure gradient in the North Atlantic. *Int. J. Climatol.*, 13, 423-436.

Bouws, E., D. Jannink and G. Komen, 1996: The increasing wave height in the North Atlantic Ocean. *Bull. Amer. Meteor. Soc.*, 77, 10, 2275-2277.

Cardone, V.J., J.G. Greenwood and M.A. Cane, 1990: On trends in historical marine wind data. *J. Climate*, 3, 113-127.

Cardone, V.J., A.T. Cox and V.R. Swail, 2003: Evaluation of NCEP reanalysis surface marine wind fields for ocean wave hindcasts. *Guide to the Applications of Marine Climatology, Part II*. WMO/TD-No. 1081, World Meteorological Organization. Geneva, Switzerland.

Carter, D.J.T. and L. Draper, 1988: Has the North-East Atlantic become rougher? *Nature*, 332, 494.

Cox, A.T. and V.R. Swail, 2001: A global wave hindcast over the period 1958-1997: validation and climate assessment. *J. Geophys. Res.*

Cox, A.T., V.J. Cardone and V.R. Swail, 2003: On the use of in situ and satellite wave measurements for evaluation of wave hindcasts. *Guide to the Applications of Marine Climatology, Part II*. WMO/TD-No. 1081, World Meteorological Organization. Geneva, Switzerland.

Gulev, S.K. and L. Hasse, 1999: Changes of wind waves in the North Atlantic over the last 30 years. *Int. J. Climatol.*, 19, 1091-1018.

Kushnir, Y., V.J. Cardone, J.G. Greenwood and M.A. Cane: 1997: The recent increase in the North Atlantic wave height. *J. Climate,* 10, 2107-2113.

Schmidt, H. and H. von Storch, 1993. German Bight storms analyzed. *Nature*: 365:791.

Sterl, A., G.J. Komen and P.D. Cotton, 1998: Fifteen years of global wave hindcasts using winds from the European Centre for Medium-range Weather Forecasts reanalysis: validating the reanalyzed winds and assessing the wave climate. *J. Geophys. Res.* 103 (C3), 5477-5492.

Swail, V.R. and A.T. Cox, 1999: On the use of NCEP/NCAR reanalysis surface marine wind fields for a long-term North Atlantic wave hindcast. *J. Atmos. Ocean. Technology,* 17, 532-545.

Wang, X.L. and V.R. Swail, 2001: Changes of extreme wave heights in Northern Hemisphere oceans and related atmospheric circulation regimes. *J. Climate,* 14.

Wang, X.L. and V.R. Swail, 2002: Trends of Atlantic wave extremes as simulated in a 40-year wave hindcast using kinematically reanalyzed wind fields. Submitted to *J. Climate*.

Wang, X.L., F.W. Zwiers and H. von Storch, 1999: Using redundancy analysis to improve dynamic seasonal mean 500 hPa geopotential forecasts. *J. Climate*.

WASA Group, 1998: Changing waves and storms in the northeast Atlantic? *Bull. AMS*, 79(5):741-760.

White, G. H., 2000: Long-term trends in the NCEP/NCAR Reanalysis. *Proc. Second WCRP International Conference on Reanalyses*. WCRP-109, WMO/TD-No. 95. World Meteorological Organization. Geneva, Switzerland. 54-57.